International Journal of Marine Energy 3–4 (2013) e11–e25

Contents lists available at ScienceDirect

International Journal of Marine Energy

journal homepage: www.elsevier.com/locate/ijome

Optimal siting of offshore wind-power combined with wave energy through a marine spatial planning approach

Arianna Azzellino [a,*], Vincenzo Ferrante [b], Jens Peter Kofoed [c], Caterina Lanfredi [a], Diego Vicinanza [b]

[a] Civil and Environmental Engineering Department, Politecnico di Milano, Piazza Leonardo da Vinci, 32, 20133 Milano, Italy
[b] Dipartimento di Ingegneria Civile, Design, Edilizia e Ambiente, Seconda Università degli Studi di Napoli, Via Roma 29, 81031 Aversa (Caserta), Italy
[c] Department of Civil Engineering, Aalborg University, Sohngaardsholmsvej 57, Aalborg DK-9000, Denmark

ARTICLE INFO

Keywords:
Marine spatial planning
Combined wind and wave energy
North sea
Environmental impact
Optimal siting

ABSTRACT

Recently has been suggested by some authors that resource diversity may be used to manage the variability of renewable power and lower the system integration costs of renewables. The key benefit, deriving from the diversification of the mix of renewable technologies, lies in the possibility of reducing the variability of the produced power. As MREIs develop, it is likely to result in further transformation of coastal seas, already affected by significant pressure from human activities. In this perspective, both the potential for combining different renewable technologies, and the impact associated to such development should be considered in the context of the existing pressures. The spatial conflicts of sea uses and the demand for sea space are in fact increasingly growing and quantitative MSP criteria may help to evaluate the sustainability of conflicting human activities in the perspective of the minimization of the overall environmental impacts. In this study the opportunity of co-locating offshore wind turbines and wave energy converters is analyzed through a MSP approach.

* Corresponding author. Tel.: +39 23996431.
E-mail addresses: arianna.azzellino@polimi.it (A. Azzellino), jpk@civil.aau.dk (J.P. Kofoed), caterina.lanfredi@polimi.it (C. Lanfredi), diego.vicinanza@unina2.it (D. Vicinanza).

2214-1669/$ - see front matter
http://dx.doi.org/10.1016/j.ijome.2013.11.008

Introduction

Marine renewable energy installations (MREIs) are likely to become a large part of the future energy mix worldwide. Recently has been suggested by some authors [10,13] that resource diversity may be used to manage the variability of renewable power and lower the system integration costs of renewables. The key benefit, deriving from the diversification of the mix of renewable technologies, lies in the possibility of reducing the variability of the produced power. When adopting a single variable source (for example wind) the only way to reduce variability is by geographical diversity and displacement of the farms. When considering different variable sources, if they are uncorrelated, their combination is a powerful alternative in order to obtain a reduction of the overall variability of the produced power. On the other hand, the increasing awareness of the cumulative effects of human activities on the marine ecosystem and the rapid development of the offshore renewable energy sector has led to an increased requirement for marine spatial planning (MSP) to fulfill the need of a holistic and integrated approach to management [4,3]. As MREIs develop, it is likely to result in further transformation of our coastal seas, already affected by significant pressure from human activity. In this perspective, both the potential for combining different renewable technologies, and the impact associated to such development should be considered in the context of the existing pressures. Spatial planning approaches to marine areas are increasingly required and a distinct field of study and practice is emerging as the result of this new awareness [6,7,12]. The spatial conflicts of sea uses and the demand for sea space are in fact increasingly growing. The development of the MRE sector in such a complex framework of existing uses, pressures and foresees developments, makes the need for MSP even more urgent. Spatial decision support systems, through the efficient exchange of information between experts, stakeholders and decision makers offer the opportunity to guide the transition from the single sector management toward the integrated management of sea uses. The early prediction of the areas of potential conflicts creates the ground for mitigation actions or early negotiations between stakeholders. In this study the opportunity of co-locating offshore wind turbines and wave energy converters is analyzed through a MSP approach.

Study area

The Danish portion of the North Sea provides a good case study for illustrating the complexity of issues at play in the dimensions of maritime spatial planning. Quantitative MSP criteria are, in fact, requested to evaluate the sustainability of conflicting human activities in the perspective of minimizing the overall environmental impacts. The North Sea is, in fact, under large anthropogenic pressure since a multitude of human activities, both on the sea itself and its catchment contribute to the environmental impact affecting the area.

Offshore human activities include intensive marine traffic, industrial fisheries, construction and operation of technical installations such as offshore oil platforms, wind power farms, cables and pipelines. The advantages in combining the power production of wave converters and offshore wind turbines has been recently examined at Hanstholm, located on the North-West coast of Jutland, Denmark [8]. The opportunities of providing a smooth and continuous power output are investigated. The study is based on simultaneous, real power productions from Wavestar wave converter and a 525 kW wind turbine of the Nordic Folkecenter, at Hanstholm, Denmark. It examines the metocean conditions at the site and the relationship between the wind and the wave resource, and analyses the power productions of the wave converter and the wind turbine working individually and in combinations according to five different scenarios.

Methods

The fact that waves are more constant than winds and the delay between both resources provides the background of this study. We used the ECMWF 40 (ERA-40) Global Wave Forecast Data Set (http://www.ecmwf.int/).

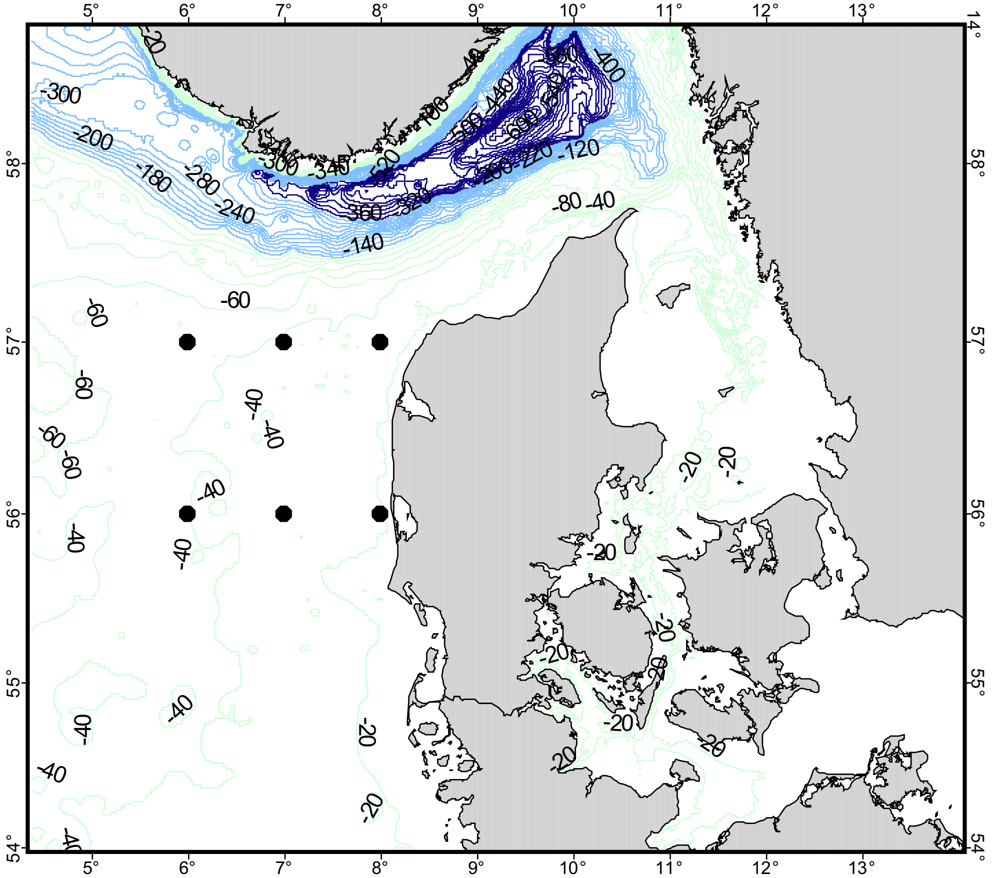

Fig. 1. Study area. The ECMWF stations of the Global Wave Forecast Data Set (ERA-40) are also shown (black dots).

The ECMWF is a meteorological data assimilation project, in which historical observational data spanning an extended period is implemented through a single consistent analysis in forecast models. These operational, numerical weather predictions are used to predict meteorological future states, based on how the climate system evolves with time from an initial state. The ECMWF data set is composed of a coupled ocean atmosphere, general circulation model, i.e. an atmospheric reanalysis coupled with a wave model integration where no wave parameters are assimilated, making the wave part a hindcast run. The fields available from this dataset are wind speed at 10 m, mean direction of total swell, and wind waves, mean period of total swell, and wind waves, mean wave direction, mean wave period, mean wave period based on first moment, mean wave period based on first

Table 1
Relationships of the main parameters with bathymetry that have been used for the spatial interpolation.

	Wind speed, v_w	Wave period, T_z	Significant wave height, H_s
Coefficients	b_0: 7.135	b_0: 5.788	b_0: 1.542
	b_1: .0.028*D	b_1: −0.011*D	b_1 −0.005*D
R^2	0.741	0.697	0.765

* D: depth.

Table 2
Main Statistics of the wind and wave parameters.

		Wind speed (m/s)	Mean wave direction (m asl)	Mean wave period (m asl)	Significant wave height (m asl)
N		256,676	256,676	256,676	256,676
Mean		9.07	233.60	6.44	2.01
Median		9.12	252.13	6.39	1.85
Std. deviation		3.86	83.63	1.33	1.14
Minimum		.01	.00	2.58	.10
Maximum		29.52	359.99	13.09	10.18
Percentiles	10	3.95	99.47	4.74	.71
	20	5.49	159.10	5.25	.97
	25	6.15	192.14	5.46	1.10
	30	6.79	211.09	5.67	1.24
	40	7.98	232.82	6.04	1.54
	50	9.12	252.13	6.39	1.85
	60	10.18	271.99	6.74	2.16
	70	11.21	292.21	7.11	2.48
	75	11.77	301.16	7.32	2.67
	80	12.38	309.14	7.56	2.89
	90	14.02	322.65	8.19	3.53

moment for swell, mean wave period based on first moment for wind waves, mean wave period based on second moment, mean wave period based on second moment for swell, mean wave period based on second moment for wind waves, peak period of 1D spectra, significant height of total swell, significant height of wind waves, significant wave height, wave spectral directional width, wave spectral

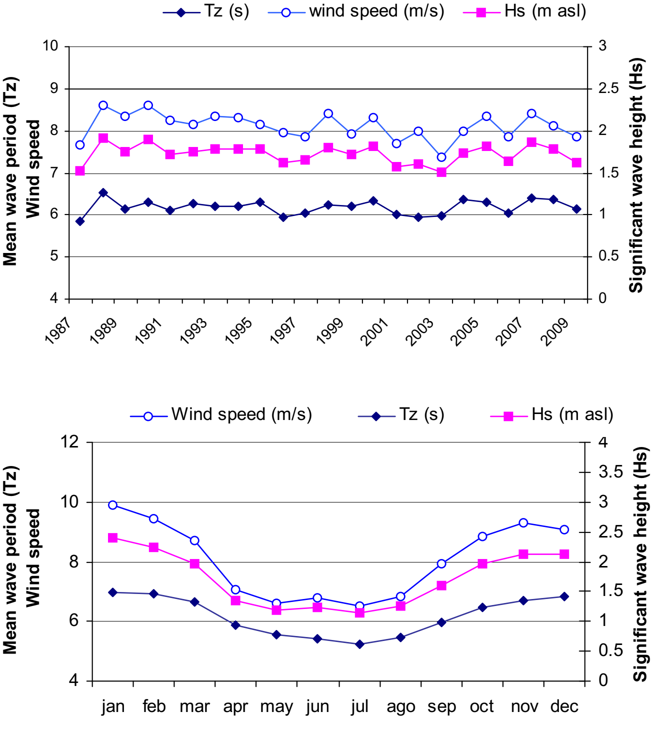

Fig. 2. Meteoclimatic conditions in the study area. The upper chart shows the inter-annual variability while the lower chart shows the seasonality.

Table 3
Wind and wave correlations with time.

		Year	Wind speed	Significant wave height	Mean wave period
Year	Pearson correlation	1	−.020**	−.008**	.030**
	Sig. (2-tailed)		.000	.000	.000
	N	387,306	387,306	193,584	193,584
Wind speed	Pearson correlation	−.020**	1	.863**	.447**
	Sig. (2-tailed)	.000		.000	.000
	N	387,306	387,306	193,584	193,584
Significant wave height	Pearson correlation	−.008**	.863**	1	.769**
	Sig. (2-tailed)	.000	.000		.000
	N	193,584	193,584	193,584	193,584
Mean wave period	Pearson correlation	.030**	.447**	.769**	1
	Sig. (2-tailed)	.000	.000	.000	
	N	193,584	193,584	193,584	193,584

** Correlation is significant at the 0.01 level (2-tailed).

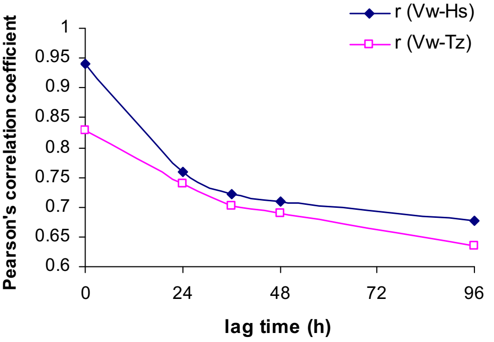

Fig. 3. Pattern of the wind-wave correlations as function of lag time. *Vw*: wind speed; *Hs*: significant wave height; *Tz* mean wave period.

Table 4
Factor loadings of wind and wave data with respect to the extracted components.

	Principal components	
	PC1	PC2
U wind component	.656	−.476
V wind component	−.161	.592
Wind speed	.757	.497
Mean wave direction	.421	−.796
Mean wave period	.820	.056
Significant wave height	.917	.350

Extraction method: Principal Component Analysis.

directional width for swell, wave spectral directional width for wind waves. We used the measurements available at the stations 56°–6°, 56°–7°, 56°–8° and 57°–6°, 57°–7°, 57°–8° (Fig. 1) and extracted the U and V wind components, mean wave direction, mean wave period and wave significant height. The data covered a 22-year period from 1987 to 2009. Moreover, a grid was created for the study area for the purpose of the spatial analysis, dividing the area into 300 cells of 22 × 12 km of grid size. As indicators of human pressure the ship traffic and the relevance of the area for the fisheries

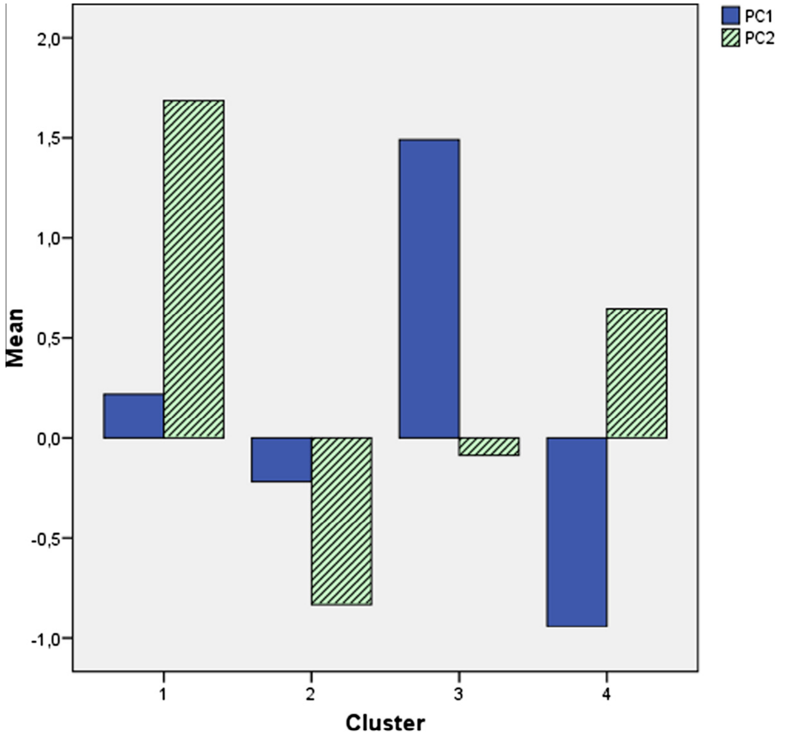

Fig. 4. Standardised characteristics of the four clusters: *cluster 1* wind and wave characteristics slightly above the average, V wind component higher than the average and lower wave direction; *cluster 2* all characteristics below the average; *cluster 3* wind and wave characteristics above the average, average V wind component and wave direction; *cluster 4* wind and wave characteristics below the average, V wind component higher than the average and lower wave direction. (For interpretation of the references to colour in this figure legend, the reader is referred to the web version of this article.)

were taken into account considering their highest impact. Ship traffic was derived from AIS data (http://www.marinetraffic.com/ais) whereas the fishery productivity of the area was evaluated in terms of biomass caught per hauling time and derived from the data publically available from the ICES Database of Trawl Surveys (DATRAS; http://datras.ices.dk). Bathymetry data were obtained through the GEBCO One minute Digital Atlas.

Data analysis

A. Wind and wave conditions

The present work has been based on the data records supplied by the ECMWF 40 (ERA-40) Global Wave Forecast Data Set. From 1987 to 2009, wind data were available every three hours and wave data every 6 h. The data consist of wind speed v_w, wave period T_z and significant wave height H_s time series. The correlation between wind and wave parameters were quantified through the Pearson's correlation coefficient:

$$r = \frac{1}{N}\sum_{k=1}^{N}\frac{[x(k)-\mu_x][y(k)-\mu_y]}{\sigma_x\sigma_y}$$

where μ_x, μ_y and σ_x, σ_y are the mean and the standard deviation of x and y. The Pearson's coefficient may also be use to give the correspondence between wind and wave, after a certain a time lag τ. In this study, we were particularly interested in assessing the instantaneous correspondence between wind and wave power at the different locations.

However we considered also different lag times to evaluate the average delay between wind and wave.

B. Classification of the meteoclimatic conditions

Two different multivariate techniques were used to analyse wave energy data and the final multi criteria matrix: Principal Component Analysis and Cluster Analysis [2].

Table 5
Cluster characteristics in terms of the main statistics of wind and wave data.

Cluster		U wind component	V wind component	Wind speed	Mean wave direction	Mean wave period	Significant wave height
1	Mean	−3.994	6.567	12.034	152.799	6.613	2.543
	Median	−5.625	8.451	11.654	159.375	6.540	2.364
	Std. Deviation	7.158	6.321	2.333	61.018	.781	.726
	Minimum	−27.492	−18.040	2.679	.012	4.633	1.071
	Maximum	15.305	27.046	29.522	359.674	10.727	7.439
	N	24,854	24,854	24,854	24,854	24,854	24,854
2	Mean	3.580	−1.283	5.879	292.112	5.935	1.189
	Median	4.046	−1.334	5.863	298.730	5.855	1.156
	Std. Deviation	3.578	3.678	2.497	35.278	1.091	.491
	Minimum	−11.944	−14.465	.007	114.128	2.647	.099
	Maximum	12.533	8.842	15.349	359.989	12.735	3.197
	N	83,307	83,307	83,307	83,307	83,307	83,307
3	Mean	9.599	−1.750	12.106	280.097	7.683	3.135
	Median	9.820	−1.866	11.910	279.699	7.573	2.888
	Std. Deviation	3.787	6.659	2.708	32.790	.996	.962
	Minimum	−11.453	−20.020	1.224	168.766	5.149	.999
	Maximum	25.092	17.650	29.026	359.993	13.090	10.184
	N	38,238	38,238	38,238	38,238	38,238	38,238
4	Mean	−2.683	2.876	6.638	140.062	5.127	1.064
	Median	−3.284	3.645	6.792	142.654	5.102	1.054
	Std. Deviation	4.059	4.035	2.040	70.784	.787	.391
	Minimum	−2.683	−10.462	.157	.000	2.585	.099
	Maximum	10.087	11.848	12.789	347.129	8.927	2.648
	N	47,185	47,185	47,185	47,185	47,185	47,185
Total	Mean	2.270	.646	8.084	234.791	6.170	1.716
	Median	3.124	.652	7.797	254.796	6.056	1.463
	Std. Deviation	6.427	5.668	3.694	85.539	1.306	1.049
	Minimum	−27.492	−20.020	.007	.000	2.585	.099
	Maximum	25.092	27.046	29.522	359.993	13.090	10.184
	N	193,584	193,584	193,584	193,584	193,584	193,584

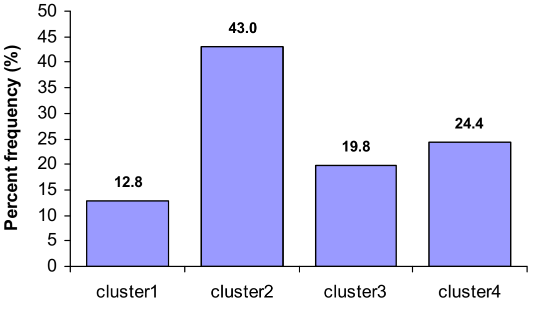

Fig. 5. Frequency distribution of the four clusters.

Table 6
Main statistics of the logistic regression model: model coefficients, standard errors and level of significance of the coefficients corresponding to the Wald statistic.

	B	S.E.	Wald	df	Sig.	Exp(B)	95% C.I. for EXP(B)	
							Lower	Upper
Significant wave height	−7.061	.036	37,792	1	.000	.001	.001	.001
Constant	13.263	.069	37,216	1	.000			

(1) Principal Component Analysis

Principal Component Analysis (PCA) was chosen to reduce the dimensionality of the wind and wave statistics. PCA extracted the eigenvalues and eigenvectors from the covariance matrix of the original variances. The number of factors to retain was chosen on the basis of the "eigenvalue higher than 1" criterion (i.e. all the factors that explained less than the variance of one of the original variables were discarded). That allowed to select few components to describe the whole data set with minimum loss of original information.

(2) K-means Cluster Analysis

A K-means Cluster Analysis (CA) [2] was used to analyse the similarities of data groups. As distance measure, the Euclidean Distance was chosen:

$$d_2(\mathbf{x}_i, \mathbf{x}_j) = \sqrt[2]{\sum_{k=1}^{q} (\mathbf{x}_{ik} - \mathbf{x}_{jk})^2}$$

The k-means CA was run twice. The second time the cluster centroids of the final solution of the first run were used as initial centers of the second run.

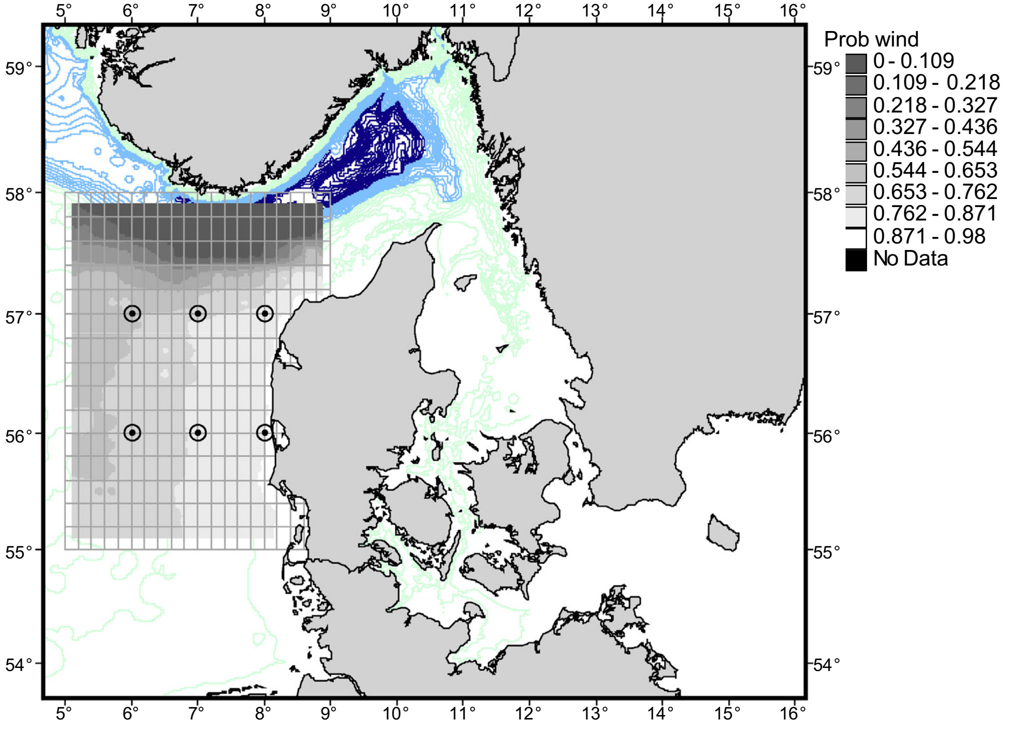

Fig. 6. Clusters 2 + 4 probability: lighter colour shows the area with higher occurrence probability of clusters 2 + 4 conditions (i.e. wind and waves uncorrelated).

A. Spatial interpolation

AIS data on ship traffic and DATRAS data of catch weigths were both interpolated using a Inverse Weighted Distance interpolator (IWD).

Wind and wave data were interpolated through linear regressions as function of bathymetry. Table 1 shows the regression coefficients used for the interpolation.

A. Prediction of the optimal conditions

A binary logistic regression analysis [2,11] was used to predict the optimal conditions to combine wave and wind energy (i.e. the class where the two are uncorrelated). A weighting factor was applied to balance the number of cases with optimal conditions with the cases where wind and waves were correlated. In order to select the best set of predictors, a forward stepwise method was used. So each predictor was tested for entry into the model, one by one, based on the significance level of the Wald statistic [11]. After each entry, variables that were already in the model were tested for possible removal. The procedure stopped when no more variables met entry or removal criteria or when the current model was the same as the previous.

Results

Wind and wave conditions

Table 2 presents the main statistics of the wind and wave parameters throughout the study period (1987–2009).

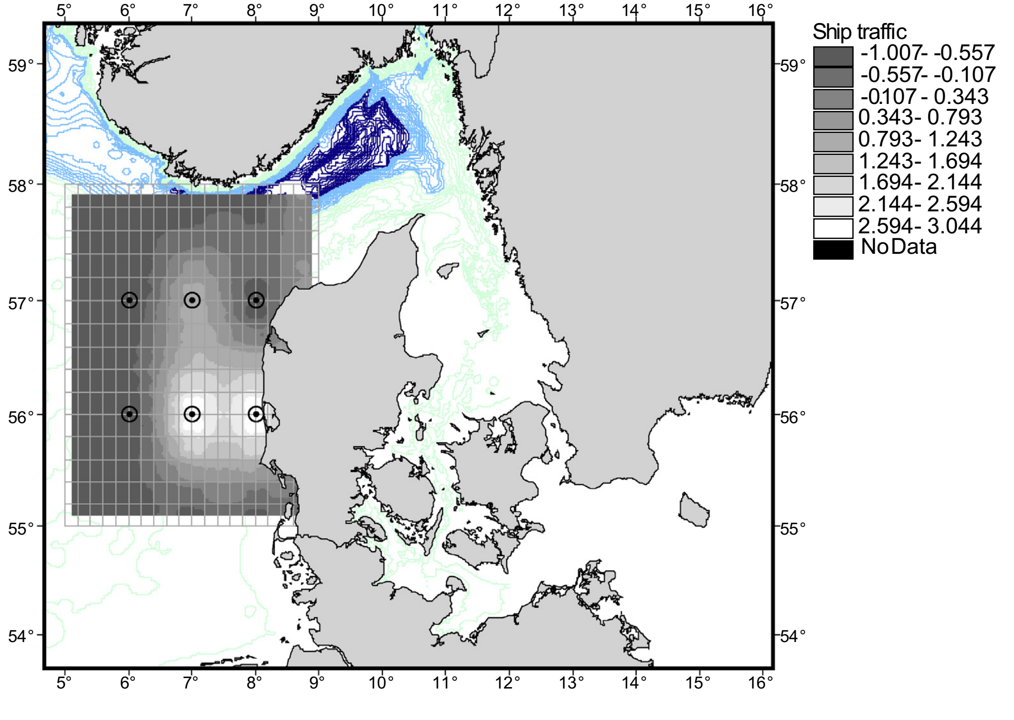

Fig. 7. Ship traffic: the areas of intense naval traffic are shown in lighter colours. (For interpretation of the references to colour in this figure legend, the reader is referred to the web version of this article.)

As it can be observed in Fig. 2 the area is characterized by a modest inter-annual variability and a strong seasonality of the meteoclimatic conditions. Table 3 shows the correlations among the wind and wave parameters. The same correlations were found in all the six considered ECMWF stations.

Moreover, the same correlations were evaluated at different lag times to analyse the average delay between wind and wave. Fig. 3 shows the pattern of these correlations as function of lag time.

This pattern suggests that, although wind and waves are generally well correlated, there might be conditions when the two are largely uncorrelated and these conditions are the most interesting in the perspective of reducing the overall variability of the produced power. So in order to identify those patterns, the different meteoclimatic conditions were classified by means of the k-mean CA algorithm.

Classification of the meteoclimatic conditions

PCA was applied to the wind and wave data (i.e. U and V wind components, the resulting wind speed, the wave direction, period and significant height). Two components were extracted explaining the 71.7% of the original variance, the first component explaining the 45.3% and the second the 26.4%. Table 4 shows the factor loadings of the PCA solution.

The K-means Cluster Analysis was applied to the principal component scores of the meteoclimatic characteristics. A four clusters solution was chosen. Fig. 4 shows the four clusters characteristics in terms of the principal component scores.

As Table 5 shows, the four clusters present different meteoclimatic characteristics:

– *cluster 1:* average wind (v_w: 12 m/s) and wave (T_z: 6.6 s; H_s: 2.5 m asl) characteristics, V wind component higher than the average (V: 6.6 m/s) and SSE wave direction (153 deg);

– *cluster 2:* wind (v_w: 5.9 m/s) and wave (T_z: 5.9 s; H_s: 1.2 m asl) characteristics below the average, V wind component below the average (V: −1.3 m/s) and NWW wave direction (292 deg);

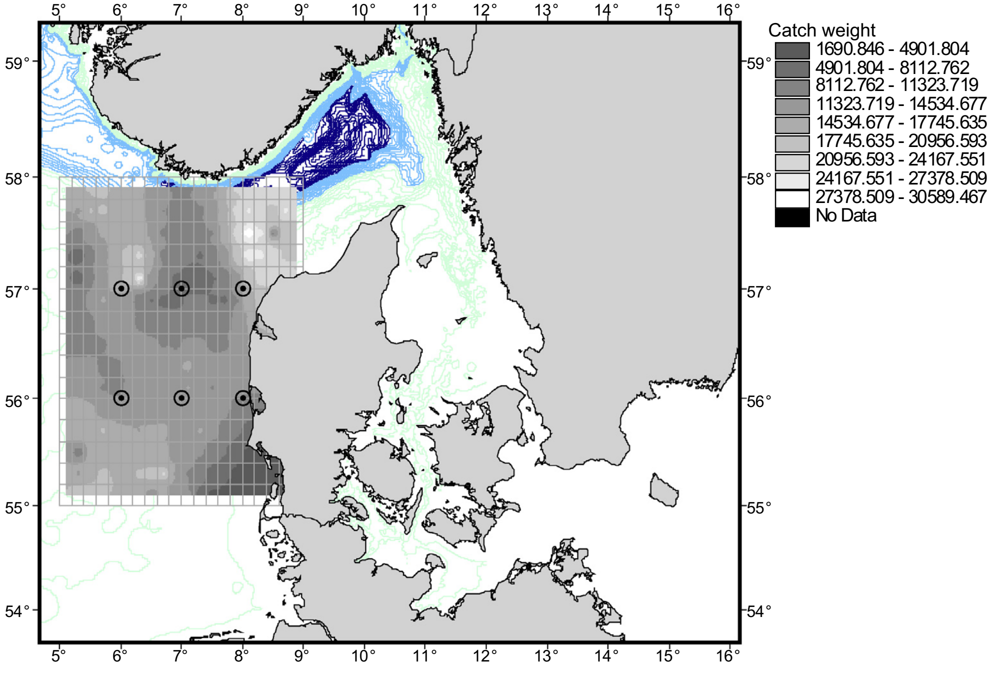

Fig. 8. Map showing the fishery productivity of the area in terms of catch weight. Lighter areas are the one with higher catch weight.

– *cluster 3:* wind (v_W: 12.1 m/s) and wave (T_z: 7.7 s; H_s: 3.1 m asl) characteristics above the average, average V wind component (V: −1.7 m/s) and NWW wave direction (280 deg);

– *cluster 4:* wind (v_W: 6.6 m/s) and wave (T_z: 5.1 s; H_s: 1.0 m asl) characteristics below the average, V wind component higher than the average (V: 2.9 m/s) and SE wave direction (140 deg).

Fig. 5 shows the frequency distribution of the four clusters. *Clusters 1* and *3* conditions, when wind and waves are correlated, occur in the 32% of the cases; *clusters 2* and *4* in the 67% of the cases.

Prediction of the optimal conditions

In the perspective of combining wind and wave energy, the optimal conditions can be identified in the wind-wave climate of the *clusters 2* and *4*. Although slightly different the two situations can be pooled together. On the other hand clusters 1 and 3 include the cases when wind and waves are strongly correlated. The binary logistic regression analysis was used to predict the probability of *clusters*(2 + 4) and *clusters*(1 + 3*)* conditions. The stepwise regression analysis selected the significant wave height as the strongest predictor. The model overall accuracy was 93%. Table 6 shows the logistic regression coefficients.

Spatial analysis

Spatial analysis was conducted by means of the grid 22 × 12 km of mesh size. For every cell of the grid the wave and wind characteristics are interpolated and the probability of the *clusters*(2 + 4) estimated through the logistic model (Fig. 6).

Figs. 7 and 8 show respectively ship traffic and fishery catch weights.

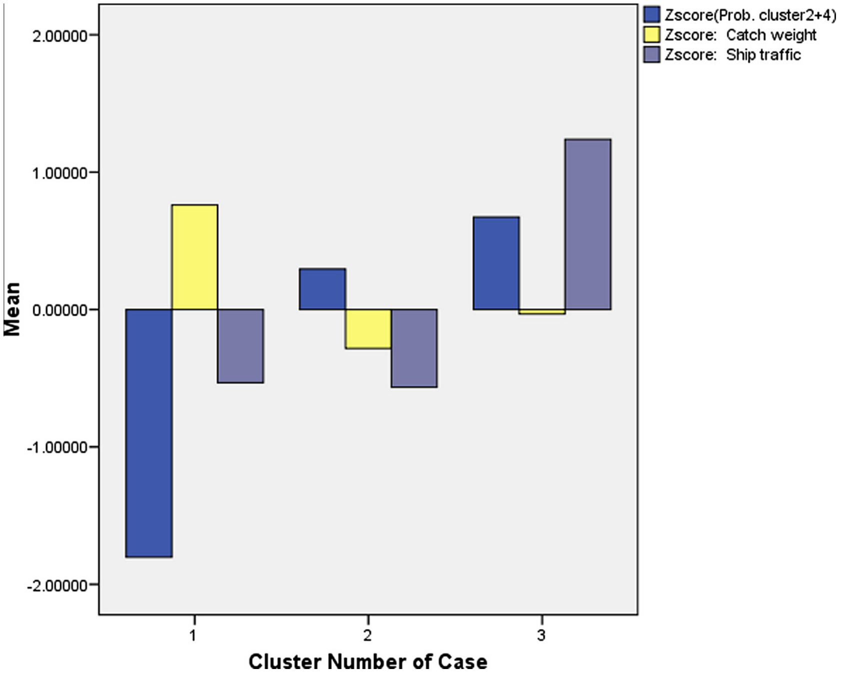

Fig. 9. Cluster characteristics for the optimal siting: the cluster which presents the conditions most suitable for the combination of wind and wave energy is the cluster 3.

Optimal siting

Figs. 6–8 suggest a potential conflict between the optimal siting of potential wind-wave combined installations and ship traffic. The areas with the higher occurrence of favourable conditions (i.e. *clusters* 2 + 4, Fig. 6) overlap with areas of intense naval traffic. On the other hand, no such a pattern was observed for fishery relevance since the catch weights tend to be homogeneous within the study area. To support the optimal siting of the wind-wave farms, a new K-means Cluster Analysis was applied to the standardized scores of the ship traffic, catch weight and occurrence probability of *clusters* 2 + 4. A three clusters solution was chosen. Fig. 9 shows the three clusters characteristics.

– *cluster 1:* catch weights above the average, lower occurrence of favourable conditions and ship traffic below the average.

– *cluster 2:* occurrence of favourable conditions above the average and catch weights and ship traffic below the average.

– *cluster 3* higher occurrence of favourable conditions, catch weights and ship traffic below the average.

These results suggest that the most interesting areas for installing combined wave and wind energy conversion systems may be the areas grouped in cluster 3. These areas have in fact a higher frequency of uncorrelated wind and wave conditions and have a lower relevance for the ship traffic and the fisheries (see Table 7).

Table 7
Favourable areas for combined wind–wave parks: higher frequency of uncorrelated wind and wave conditions and lower relevance for ship traffic and fisheries.

Cluster		Wind speed (m/s)	Wave period (s)	Significant wave height (m asl)	Zscore: Catch weight mean	Zscore: Ship traffic mean	Prob. cluster 2 + 4
1	Mean	13.483	8.282	2.676	.761	−.533	.103
	Median	12.414	7.862	2.485	.620	−.648	.014
	Std. Deviation	3.555	1.397	.635	1.010	.405	.166
	Minimum	8.385	6.279	1.765	−.712	−1.007	.000
	Maximum	21.234	11.327	4.060	3.329	.982	.690
	N	59	59	59	59	59	59
2	Mean	8.143	6.184	1.722	−.283	−.566	.720
	Median	8.322	6.254	1.754	−.204	−.769	.706
	Std. Deviation	.696	.273	.124	.942	.410	.126
	Minimum	5.758	5.247	1.296	−2.186	−1.066	.372
	Maximum	9.433	6.691	1.952	2.219	.494	.984
	N	148	148	148	148	148	148
3	Mean	7.618	5.978	1.628	−.033	1.238	.832
	Median	7.872	6.077	1.674	−.125	.988	.809
	Std. Deviation	.604	.237	.108	.829	.795	.081
	Minimum	5.915	5.309	1.324	−1.822	.080	.627
	Maximum	8.605	6.366	1.805	1.757	3.061	.980
	N	93	93	93	93	93	93
Total	Mean	9.030	6.533	1.880	.000	.000	.633
	Median	8.244	6.224	1.740	−.063	−.332	.726
	Std. Deviation	2.779	1.092	.496	1.000	1.000	.294
	Minimum	5.758	5.247	1.296	−2.186	−1.066	.000
	Maximum	21.234	11.327	4.060	3.329	3.061	.984
	N	300	300	300	300	300	300

Fig. 10 shows for each cell unit the distance from the cluster 3 centroid in a graduated colour scale, ranging from white to grey.

Greater distances from centroid (i.e. cells more distant from cluster 3 characteristics) are darker, smaller distances (i.e. cells very close to cluster 3 characteristics) are shown in light grey or white. Therefore, the light grey–white areas on the map are the most interesting for combining wind and wave energy. Fig. 11 shows the frequency of the four wind-wave patterns at ECMWF station 57°–7° which lies in a suitable area for combining wind and wave energy.

It can be observed that the clusters 2 and 4 pattern occurs more frequently in the spring–summer period. Table 8 shows the main wind and wave statistics and the corresponding available raw power according to the following expressions, respectively after [9,14]:

$$P_{wind} = \frac{1}{2}\rho_a v_w^3 \left[\frac{W}{m^2}\right]$$

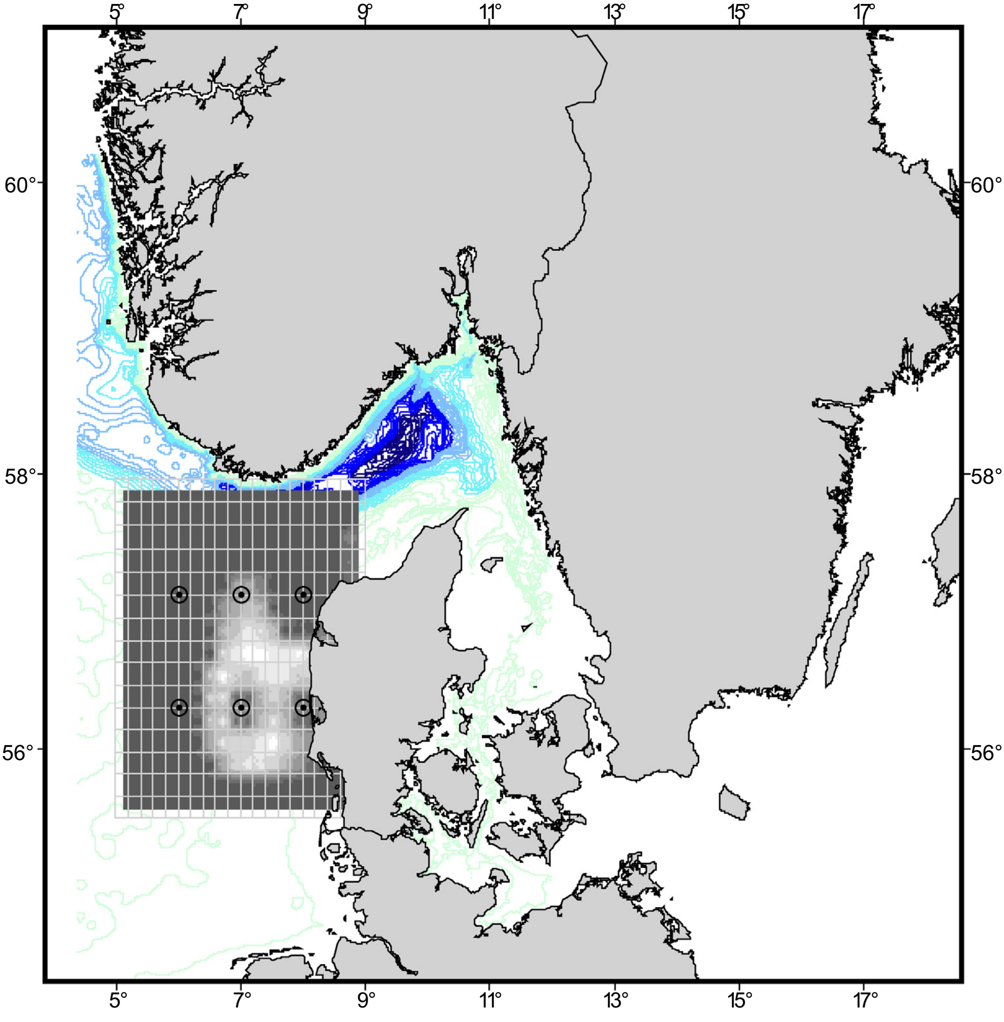

Fig. 10. Areas in light colours are the ones more suitable for combining wind and wave energy. (For interpretation of the references to colour in this figure legend, the reader is referred to the web version of this article.)

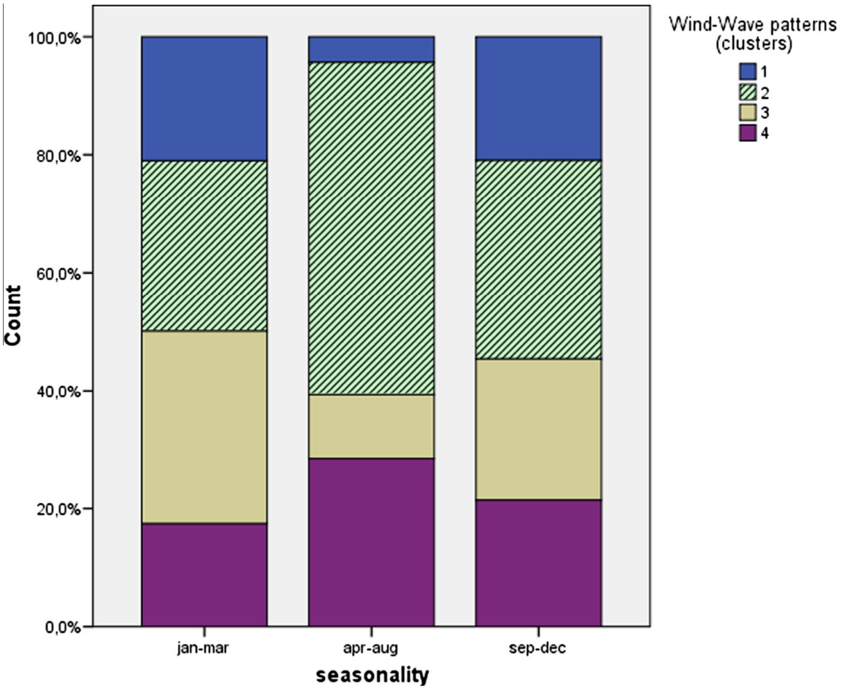

Fig. 11. Frequency of the four wind-wave clusters at the ECMWF station 57°–7°. (For interpretation of the references to colour in this figure legend, the reader is referred to the web version of this article.)

where v_w is the wind speed, and ρ_a is the air density, assumed as equal to 1.23 kg/m^3, considering an average air temperature of 5 °C.

$$P_{wave} = \frac{\rho_w g^2 H_s^2 T_e}{64\pi}\left[\frac{W}{m}\right]$$

where ρ is the sea water density ($\rho_{salt\ water}$ was assumed equal to 1027 kg/m^3 considering an average water salinity concentration of 33 ppm and an average water temperature of 7 °C), g is the gravity acceleration (g = 9.82 m/s^2), H_s is wave height, and T_e is the energy period.

T_e is known as the energy period defined in terms of spectral moments as:

$$T_e = \frac{m_{-1}}{m_0}$$

The energy period T_e is rarely specified and must be estimated from other variables when the spectral shape is unknown [5].

Table 8
Wind and wave statistics and corresponding raw power available characterising the cluster 2 and 4 pattern.

Statistics	Wind speed (m/s)	Wave direction (deg)	*Te* (s)	*Hs* (m asl)	P_{wind} (W/m^2)	P_{wave} (W/m)
Mean	7.07	241.7	6.318	1.234	216	4741
Median	6.84	266.7	6.195	1.067	196	3476
Std. deviation	3.18	82.3	1.212	0.717	20	307
Minimum	0.04	0.0	3.103	0.105	0.0	17
Maximum	25.35	360.0	12.095	5.645	9973	189,947
25 Percentile	4.72	209.4	5.441	0.709	64	1348
50 Percentile	6.84	266.7	6.195	1.067	196	3476
75 Percentile	9.21	305.3	7.099	1.593	478	8878

In this study it is assumed a standard JONSWAP spectrum with a peak enhancement factor of $\gamma = 3.3$ Under this assumption $T_e = 1.14$ Tz [1].

Conclusions

This study highlights the potential benefits of combining wave and wind power in the Danish North sea. The hypothesis of the diversification of renewable energies is grounded on two key benefits: (1) the variability of the produced power can be decreased, and (2) the power availability can be increased. These benefits are greater when un-correlated resources are combined. This study showed that, although waves and winds are strongly correlated, waves may have several hours of delay to winds and, in some conditions their correlation with winds may be lower. In these situations the combined production would be less variable and more available.

This pattern in the Danish North sea occurs more frequently closer to the coast and during the spring-summer period. Moreover, the study shows how quantitative spatial planning methods may support the selection the sites of potential interest in the perspective of co-locating wind and wave energy installations. The presented spatial analysis allowed also the early identification of potentially conflictual uses (i.e. ship traffic and fisheries) and provided support for the optimal siting of the wind-wave parks in the light of the environmental sustainability.

Acknowledgment

The work described in this paper was partially supported by the EC FP7 Marie Curie Actions People, Contract PIRSES-GA-2011-295162 – ENVICOP project (Environmentally Friendly Coastal Protection in a Changing Climate) and by RITMARE Flagship Project (National Research Project funded by the Italian Ministry of University and Research).

References

[1] ABP Marine Environmental Research Ltd. (2004) Atlas of UK Marine Renewable Energy Resources: Technical Report, Report No. R.1106 prepared for the UK Department of Trade and Industry.
[2] A. Afifi, V. Clark, in: Computer-Aided Multivariate Analysis, fourth ed., Texts in Statistical Science, Chapman & Hall/CRC Press, 1996.
[3] Azzellino, A., Conley, D., Vicinanza, D., Kofoed, J.P. Marine renewable energies: Perspectives and implications for marine ecosystems. The Scientific World Journal, 2013, art. no. 547563.
[4] H. Backer, Transboundary maritime spatial planning: a Baltic Sea Perspective, J. Coast. Conserv. 15 (2011) 279–289.
[5] Cornett A.M. A global wave energy resource assessment. In: Proceedings of the 18th International Conference ISOPE, Vancouver, BC, Canada, 2008.
[6] F. Douvere, C. Ehler, Introduction, Mar. Policy 32 (2008) 759–761.
[7] Ehler C, Douvere F. Marine spatial planning: a step-by-step approach toward ecosystem-based management. Intergovernmental oceanographic Commission and Man and the Biosphere programme. IOC Manuals and Guides 53 ICAM Dossier 6. UNESCO, Paris, 2009, p. 99.
[8] Fernández Chozas J., Kramer M.M., Sørensen H.C., Kofoed J.P. 2012. Combined Production of a full-scale Wave Converter and a full-scale Wind Turbine – a Real Case Study. Proc. of the 4th International Conference on Ocean Energy, 17 October, Dublin., 2012.
[9] L. Freris, D. Infield, Renewable Energy in Power Systems, John Wiley & Sons Inc., 2008.
[10] F. Fusco, G. Nolan, J.V. Ringwood, Variability reduction through optimal combination of wind/wave resources – An irish case study, Energy 35 (2010) 314–325.
[11] D.W. Hosmer, S. Lemeshow, Applied Logistic Regression, 2nd ed., John Wiley & Sons, New York, 2000.
[12] S. Jay, Built at sea: marine management and the construction of marine spatial planning, Town Plan. Rev. 81 (2) (2010) 173–191.
[13] E.D. Stoutenburg, N. Jenkins, M.Z. Jacobson, Power output variations of co-located offshore wind turbines and wave energy converters in California, Renewable Energy 35 (2010) 2781–2791.
[14] D. Vicinanza, P. Contestabile, V. Ferrante, Wave energy potential in the north-west of Sardinia (Italy), Renewable Energy 50 (2013) 506–521.